Supplement of Constraining pesticide degradation in conceptual distributed catchment models with compound-specific isotope analysis (CSIA)

Sylvain Payraudeau[1], Pablo Alvarez-Zaldívar[1], Paul van Dijk[2], and Gwenaël Imfeld[1]

[1]Institut Terre et Environnement de Strasbourg (Université de Strasbourg, CNRS/ENGEES, ITES UMR 7063), Strasbourg, 67084, France
[2]Chambre Régionale d'Agriculture Grand Est, Espace Européen de l'Entreprise, 2 rue de Rome CS 30022 Schiltigheim, 67013 Strasbourg, France

Correspondence: Sylvain Payraudeau (sylvain.payraudeau@engees.unistra.fr)

1 Hydro-climatic conditions

Summary temperature and reference evapotranspiration, obtained from MeteoFrance (Station no. 67516001), and summary rainfall and discharge (measured) are shown in Table S1.

Table S1. Summary hydrological and climatic conditions (Alvarez-Zaldivar et al., 2018).

2016	$P(mm/d)^a$	$P_{tot}(mm)^b$	$ETP(mm/d)^c$	$T(C)^d$	$Q(mm/d)^e$	% Wet Days ^{f}
April	2.7±4.6	82.2	2.2±0.8	9.1±2.9	0.6±0.6	67%
May	4.6±7.1	136.8	3.1±1.2	14±3.2	0.9±1.3	63%
June	4.8±7.0	145.6	3.7±1.2	17.6±2.9	1.2±1.2	80%

[a] Mean daily rainfall; [b] total rainfall; [c] mean daily reference evapotranspiration; [d] mean daily temperature; [e] mean daily discharge normalised by total catchment area; [f] percent of days in a month were rainfall occurred.

2 Catchment description, sampling and transect area extents

Field data was collected from a 47 ha headwater catchment located in Alteckendorf, France (48° 47'11.03"N, 7° 35' 0.46"E) (Alvarez-Zaldivar et al., 2018; Lefrancq et al., 2018). The mean catchment slope is 6.7 ± 4.7% with an altitude ranging between 190 and 230 m.

Figure S1. Transects (weekly) and plot (1, 50 and 100 days) catchment sampling. "Other" contains roads, grass strips and orchards

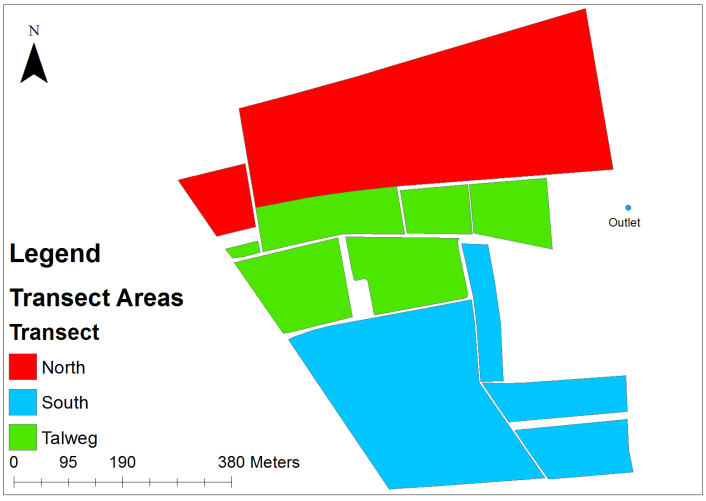

Figure S2. Delimited transect areas used to extrapolate remaining mass from soil concentrations measured for each transect sample weekly.

3 Farmer surveys

Three main applications (A1, A2, A3) were confirmed from farmer surveys and observations from weekly transect concentrations [S-metolachlor] and δ^{13}C (Fig. S7). However, these concentration increases do not correspond with a significant decrease in δ^{13}C that would be expected from a fresh application with a characteristic signature ($\delta^{13}C_0 = -32.2 \pm 0.5‰$).

Table S2. Applied mass (Kg) of active ingredient (S-metolachlor) per transect by date and days since 1^{st} application. Ranges indicates uncertainty of exact application date (Alvarez-Zaldivar et al., 2018).

App. No.	Date	Days	North	Valley	South
A1	March 20 - 25^{th}	0 - 5	5.1	1.6	11.1
A2	April 13 - 14^{th}	25 - 26	8.0	1.8	2.9
A3	May 25 - 31^{st}	67 - 73	7.2	2.4	0.0
Total (Kg)			20.2	5.9	14.0

4 Mass balance estimations

Soils. Pesticide mass along a catchment's transect area $M_{Tr,t}$ [μg] is given by:

$$M_{Tr,t} = C_{Tr,t} \cdot \rho_{b_0} \cdot A_{Tr} \cdot D \tag{1}$$

were C_{Tr} is the dry weight S-met soil concentration [$\mu g/g\ soil\ dry\ wt$] on transect Tr at time t and A_{Tr} is the associated transect area [m^2] (Fig. S2) and D is sampling depth (1 cm). A homogeneous bulk density (ρ_{b_0} = 0.99 g/cm^3) was assumed based on sample measurements obtained across the catchment.

Transect signature and pesticide mass was then used to compute bulk signatures across the catchment ($\delta^{13}C_{bulk}$) and given by:

$$\delta^{13}C_{bulk,t} = \sum_{Tr=1}^{TR=3} \frac{M_{Tr,t}}{M_{tot,t}} \delta^{13}C_{Tr,t} \tag{2}$$

were $\delta^{13}C_{Tr}$ is the S-met isotope signature in transect Tr and M_{tot} [μg] the total catchment mass at time t.

Outlet. Outlet loadings (OL) [μg] where calculated based on flow proportional samples given by:

$$OL_{ws} = C_{ws} \int_{t}^{\Delta t} V(t)dt \tag{3}$$

where C the concentration [$\mu g/L$] of water sample ws and V [L] is discharge over the sample time interval Δt [h].

5 $\delta^{13}C$ analysis

The GC-C-IRMS system consisted of a TRACE™ Ultra Gas Chromatograph (ThermoFisher Scientific) coupled via a GC IsoLink/Conflow IV interface to an isotope ratio mass spectrometer (DeltaV Plus, ThermoFisher Scientific). The carbon isotope ratios are reported in δ notation [‰], using a three-point calibration against the Vienna Pee Dee Belemnite (V-PDB) standard ($11237.2 \cdot 10^{-6}$) and given by:

$$\delta^{13}C_{sample}[‰] = \frac{R_{sample} - R_{standard}}{R_{standard}} \cdot 1000 \tag{4}$$

where R_{sample} and $R_{standard}$ are the ratios $^{13}C/^{12}C$ of sample and standard, respectively. Based on GC-IRMS linearity tests, the minimum peak amplitudes needed for accurate $\delta^{13}C$ measurements was established as about 300 mV (Alvarez-Zaldivar et al., 2018), which correspond to 10 ng of carbon injected on column.

During chemical transformation, lighter isotopes (e.g., ^{12}C) exhibit lower activation energy, generally resulting in faster reaction times relative to their heavier counterparts (e.g., ^{13}C). This leads to an enrichment of the heavier isotopologues in the non-degraded pesticide fraction remaining in environmental samples (Elsner, 2010). The resulting average isotope value (e.g.,

$\delta^{13}C$) of the non-degraded fraction can then be used to quantify degradation by following the Rayleigh distillation equation (Rayleigh, 1986). Research on legacy contaminants (Hunkeler et al., 2008; Sherwood Lollar et al., 2011) and nitrate pollution (Nestler et al., 2011; Fenech et al., 2012), have shown CSIA to be a valuable complementary line of evidence to demonstrate degradation, persistence and source identification at various temporal and spatial scales. Akin to these approaches, application of CSIA to pesticides relies on the ability to monitor changes in stable isotope composition between source(s) and outlet to quantify the extent of (bio)chemical conversion at the catchment scale.

6 Hydrological model

6.1 Conceptual model

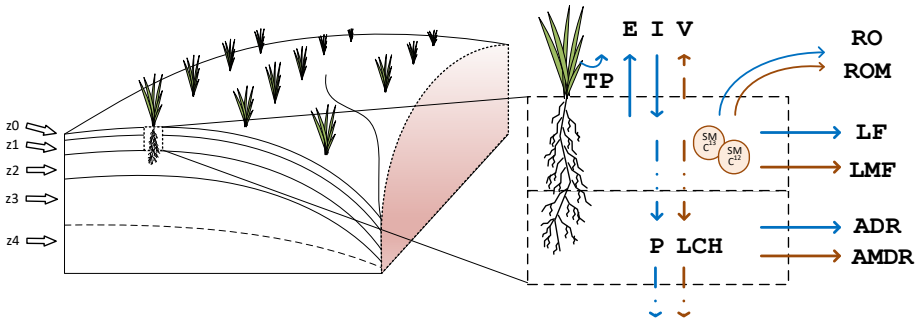

Figure S3. Conceptual 5-layer spatially distributed hydrological and reactive-transport PiBEACH model. Hydrological processes included evaporation (E), transpiration (TP), percolation (P) volatilization (V), runoff (RO), lateral flow (LF) and artificial drainage (ADR). Mass transfer processes included volatilization (V), runoff mass (ROM), lateral mass flow (LMF), leaching (LCH) and mass transfer through artificial drainage (AMDR)

6.2 Infiltration and runoff

To calculate infiltration, I (mm) and surface runoff, RO (mm), soil moisture conditions are determined by following the SCS curve number defined by the U.S. Soil Conservation Service (SCS, 1972). Infiltration is given by,

$$I = R - RO \tag{5}$$

where R (mm) is rainfall. The run-off equation is given by (Neitsch et al., 2009):

$$RO = \begin{array}{l} 0, R \leq I_a \\ \dfrac{(R-I_a)^2}{R-I_a+S}, R > I_a \end{array} \tag{6}$$

Table S3. Full set of model parameters

Parameter	Units	Bounds	95% CI	Description	Source
Layers	-	5	-	Number of model layers	Conceptual
$z0$	mm	10	-	Layer depth	"
$z1$	mm	300	-	*ibid.*	"
$z2$	mm	500	-	*ibid.*	"
$z3$	mm	zDat · (zf)	-	Depth to datum (zDat), upper water table	"
$z4$	mm	zDat · (1-zf)	-	Depth to datum (zDat), lower water table	"
z_f	-	0.75, 0.99	0.87, 0.99	z3 and z4 distribution fraction	Calibration
c_{z0z1}	d^{-1}	0, 1	0, 1	Lateral flow coefficient (Manfreda et al., 2005), z0, z1	"
c_{z2z3z4}	d^{-1}	0, 1	0.2, 0.6	*ibid.*	"
c_{adr}	d^{-1}	0, 1	0.03, 0.92	Drainage lateral flow coefficient	"
K_G	d	1100, 3650	1522, 3650	Linear reservoir constant regulating baseflow discharge	"
γ_{z0z1}	-	0, 1	0.32, 1	$log(K_{sat})$ adjustment factor for layer (z)	"
γ_{z2z3}	-	0, 1	0, 0.81	*ibid.*	"
$K_{sat,z0z1}$	mm d^{-1}	112.9, 781.8	-	Saturated hydraulic conductivity (adjusted by γ)	Agro. model
$K_{sat,z1z2z3}$		643.2	-	*ibid.*	"
θ_{WP}	-	0.19	-	Wilting point, all layers; 0.16 $\pm$ 0.03	"
$\theta_{FC,z0z1}$	-	0.37, 0.40	-	Field capacity, plow layer (0 - 300 mm); 0.37 $\pm$ 0.01	"
$\theta_{SAT,z0z1}$	-	0.49, 0.63	-	Saturation capacity, plow layer; 0.57 $\pm$ 0.04	"
$\theta_{FC,z2z3z4}$	-	0.37	-	Field capacity, z < 310 mm depth; 0.37 $\pm$ 0.03	Field charac.
$\theta_{SAT,z2z3z4}$	-	0.57	-	Saturation capacity, z < 310 mm depth; 0.57 $\pm$ 0.04	"
f_{transp}	-	0, 1	0.38, 1	Adjustment factor, transpiration	Calibration
f_{evap}	-	0, 1	0.1, 0.88	Adjustment factor, evaporation	"
$p_{bAgr,z0z1}$	g cm^{-3}	0.98, 1.36	-	Soil bulk density ; 1.17 $\pm$ 0.11	Agro. model
$p_{b,z2,z3,z4}$	g cm^{-3}	1.5	-	Soil bulk density, below plough layer; 1.5 $\pm$ 0.09	Field charac.
f_{oc}	kg kg^{-1}	0.01, 0.05	0.01, 0.05	Fraction of organic carbon (Lefrancq et al., 2018)	Calibration
K_{oc}	mlg^{-1}	0.3, 16180	0.3, 2000	Adsorption coefficient (Boitias et al., 2014; European Commission, 2004; Kollman et al., 1995; Lefrancq et al.; 2018 NCBI, 2017)	"
K_d	mlg^{-1}	0.003, 809	0.003, 76.9		"
β_{runoff}	mm	0, 1	0, 0.4	Calibration constant for runoff mass transfer (Ahuja et al., 1983)	"
K_{age}	d	0.0002, 0.07	0.0002, 0.005	Ageing rate, controls mass movement to non-bioavailable fraction	"
K_{irs}	d	0.002, 0.01	0.002, 0.009	Rate of irreversible sorption / loss of recoverable fraction	"
$DT_{50_{ref}}$	d	1, 50	9.2, 24.9	Ref. degradation half-life	"
ϵ_{iso}	-	-4.0, -1.0	-3.467, -1.721	Enrichment factor	"
β_θ	-	0, 1	0.03, 1.0	Constant exponent, degradation factor (Walker et al., 1974)	"

Parameters removed from hypercube sampling after Morris sensitivity included water content at -100 cm (W100 all layers); wilting point (all layers: θ_{WP}); field capacities ($\theta_{FC_{zX}}$) and saturation capacities (all layers: $\theta_{SAT_{zX}}$)

where I_a (mm) is the initial abstraction capacity of the surface layer, which includes surface storage, interception and infiltration prior to runoff, and typically ranges from 0.05S to 0.2S. The model adopts the latter of these values as it has provided reliable results for previous rainfall-runoff events (Lim et al., 2006). S (mm) is the retention parameter after run-off given as a function of the soil profile water content:

$$S = S_{max} \cdot \Big(1 - \frac{SW}{(SW + \exp[w_1 - w_2 \cdot SW])}\Big) \tag{7}$$

where w1 (mm) and w2 (-) are shape coefficients, SW (mm) is the soil profile water content of the first two layers, $z0$, $z1$, excluding the amount of water held in the soil profile at wilting point such that:

$$SW = max\Big[\Big\{(\frac{D_{z0}\theta_{z0} + D_{z1}\theta_{z1}}{D_{z0} + D_{z1}} - \theta_{wp}) \cdot (D_{z0} + D_{z1})\Big\}, \Big\{0\Big\}\Big] \tag{8}$$

and S_{max} (mm) is the maximum value that the retention parameter can take such that:

$$S_{max} = 254 \cdot \big(\frac{100}{CN_1} - 1\big) \tag{9}$$

Calculation of w_1 and w_2 is given by,

$$w_1 = ln\Big[\frac{FC}{(1 - \frac{S_3}{S_{max}})} - FC\Big] + w_2 \cdot FC \tag{10}$$

$$w_2 = \frac{ln\Big[\frac{FC}{(1 - \frac{S_3}{S_{max}})} - FC\Big] - ln\Big[\frac{SAT}{(1 - \frac{2.54}{S_{max}}} - SAT\Big]}{SAT - FC} \tag{11}$$

where FC (mm) is the soil profile water content at field capacity, S_3 (mm) is the retention parameter corresponding to field capacity (i.e. CN3) and SAT (mm) is the soil profile water content at saturation. S_3 is given by:

$$S_3 = 254 \cdot \big(\frac{100}{CN_3} - 1\big) \tag{12}$$

CN numbers depend on permeability, land use, slope and antecedent moisture conditions. Curve numbers are classified according to three moisture conditions: dry (wilting point - CN_1), average moisture (CN_2) and wet (field capacity - CN_3). Typical CN_2 numbers for various land covers, hydrologic conditions and soil types at a 5% slope are given in Neitsch et al. (2009). CN_2 values are used to derive CN_3 before slope adjustment,

$$CN_3 = CN_2 \cdot \exp[0.00673 \cdot (100 - CN_2)] \tag{13}$$

Before plugging eq. 13 into eq. 12, adjustment to local slope of CN_2 is required,

$$CN_{2s} = \frac{CN_3 - CN_2}{3} \cdot [1 - 2 \cdot \exp(-13.86 \cdot slope)] + CN_2 \tag{14}$$

where CN_{2s} is the curve number for average moisture conditions adjusted to the local slope. CN_1 values accounting for slope are then calculated as:

$$CN_1 = CN_{2s} - \frac{20 \cdot (100 - CN_{2s}}{\Big(100 - CN_{2s} + \exp[2.533 - 0.0636 \cdot (100 - CN_{2s})]\Big)} \tag{15}$$

Finally, recalculation of eq. 13, replacing CN_2 with CN_{2s} to adjust for local slope, is done before plugging CN_3 back into eq. 12.

6.3 Percolation

Percolation (P) is assumed to be negligible at moisture levels below field capacity. Above field capacity, percolation is given by Raes (2002):

$$P_z = D_z \tau_z (\theta_{sat,z} - \theta_{fc,z}) \frac{e^{\theta_z - \theta_{fc,z}} - 1}{e^{\theta_{sat,z} - \theta_{fc,z}} - 1}, \;\; if \; \theta_z > \theta_{fc,z} \tag{16}$$

where D_z (mm) is the soil profile depth of layer z and τ is a dimensionless drainage characteristic given by:

$$\tau = 0.0866 \cdot e^{\gamma_z \cdot log_{10}(K_{sat})}, \;\; 0 < \tau \leq 1 \tag{17}$$

where γ_z (-) is a calibration coefficient and K_{sat} (mm d^{-1}) is the saturated hydraulic conductivity.

6.4 Lateral subsurface flow

Lateral flow (LF_{z_i}) (mm) occurs when the soil moisture content exceeds the field capacity (f_{pot_i}) at each upstream cell (i) and the receiving downstream cell has available pore space capacity ($f_{cap_j} > 0$). The total flux at each cell is given by,

$$LF_{z_i} = min\Big(f_{pot_i}, f_{cap_j}\Big) \cdot D_z \tag{18}$$

$$f_{pot_i} = c_z \cdot (\theta_t - \theta_{fc}) \tag{19}$$

$$f_{cap_j} = \frac{\theta_{sat_z} - \theta_{t_z}}{\sum_{i=1}^{I}(i)} \tag{20}$$

where c_z (d^{-1}) is a subsurface flow coefficient analogous to Manfreda et al., (2005), f_{cap_j} (-) the soil water capacity of the downstream cell, $\sum_{i=1}^{I}(i)$ is the sum of upstream contributors and

6.5 Evapotranspiration

To account for evapotranspiration processes the FAO56 reference evaporation rate, ET_0 (mm), has been considered and adjusted dynamically according to crop and climate-specific factors. The approach assumes a dual crop coefficient approach

appropriate for daily time-step calculations (Allen et al., 1998) and made up of a basal crop coefficient (K_{cb}) and a soil water evaporation coefficient (K_e). Potential evapotranspiration (ET_p) is then given by

$$ET_p = K_c \cdot ET_0 \tag{21}$$

$$K_c = K_{cb} + K_e \tag{22}$$

where K_{cb} varies according to crop-specific development stage. In cases where the mean value for daily relative humidity during the mid- or late-season growth stage ($RH_{min}\%$) differs from 45% or where wind speed varies by more than 2 m/s the K_{cb} values for mid- and late-season must be adjusted according to:

$$K_{cb} = K_{cb_{mid/end}} + \Big[0.04(U_2 - 2) - 0.004(RH_{min} - 45)\Big]\Big(\frac{h_{crop}}{3}\Big)^{0.3} \tag{23}$$

$$K_e = K_{cmax} - K_{cb} \tag{24}$$

where $K_{cb_{mid/end}}$ represent the reference values for sub-humid climate and moderate wind speeds (Allen et al., 1998). $U2$ is the wind speed at a height of 2 meters (m/s), RH_{min} is the minimum relative humidity (%) and h_{crop} is crop height. The soil evaporation coefficient, K_e, and K_{cmax} (-) represents an upper limit to evapotranspiration from cropped surfaces (1.05 to 1.30) and given by Allen et al. (1998):

$$K_{cmax} = max\Big[\Big\{K_{cb} + 0.05\Big\}, \Big\{1.2 + [0.04(U_2 - 2) - 0.004(RH_{min} - 45)] \cdot (\frac{h}{3})^{0.3}\Big\}\Big] \tag{25}$$

6.6 Transpiration

To account for potential transpiration processes, water uptake by roots is considered and regulated by atmospheric demand and soil water content. When there is sufficient water in the soil, potential transpiration (T_p) equals atmospheric demand (Allen et al., 1998):

$$T_p = K_{cb} \cdot ET_0 \cdot f_{tr} \tag{26}$$

ET_0 is corrected here by including a calibration coefficient f_{tr} (-). Potential transpiration is further subject to root water uptake capacity where the maximum daily uptake $T_{p(z)}$ (mm) at each layer z is given by (Prasad, 1988):

$$T_{p(z)} = 2\Big(1 - \frac{RD_{z/2}}{RD}\Big)\Big(\frac{RD_z}{RD}\Big)T_p \tag{27}$$

where RD (mm) and RD_z (mm) are the total and the soil layer's rooting depth, respectively and $RD_{z/2}$ is the soil depth at the middle of the root extension for layer z.

When soil water is insufficient to meet atmospheric demand, actual transpiration is lower than potential transpiration and given by Allen et al. (1998):

$$T_{a(z)} = K_s \cdot T_p \tag{28}$$

$$K_s = max\Big[0, min(1, \frac{\theta_t - \theta_{wp}}{\theta_c - \theta_{wp}})\Big] \cdot f_{transp} \tag{29}$$

$$\theta_c = \theta_{wp} + (1-p)(\theta_{fc} - \theta_{wp}) \tag{30}$$

$$p = p_{tab} + 0.04(5 - ET_p) \tag{31}$$

where K_s is a transpiration reduction parameter (0-1), which depends on soil water content, θ_t (m^3/m^3) and the critical soil moisture content θ_c (m^3/m^3) that defines the transition between unstressed and stressed transpiration rate. The the fraction of total depletable soil water is given by p (-) and the depletion factor (-) p_{tab}, for $ET_p \approx 5\ mm/d$ (Allen et al., 1998)[Table no. 22].

6.7 Evaporation

Evaporation is considered only on bare surfaces and assumed to be negligible under plant cover and regulated by atmospheric deman along the first $\approx$ 0.15 m of soil (Sheikh et al., 2009). Considering the difference between actual (E_a, mm/d) and potential evaporation (E_p, mm/d) (Allen et al., 1998):

$$E_p = K_e \cdot ET_0 \tag{32}$$

$$E_a = K_r \cdot E_p \tag{33}$$

where K_r is an evaporation reduction coefficient (-) given by:

$$K_r = \frac{\theta_t - \theta_{dr}}{\theta_{fc} - \theta_{dr}} \tag{34}$$

where θ_t is soil moisture (m^3/m^3) and θ_{dr} is the moisture (m^3/m^3) of air-dry soil.

6.8 Root growth

Development of the root's depth followed that of Allen et al. (1998), which adjusts the crop's maximum root depth relative to the plant's development stage, where the total root depth D_{root} is given by,

$$RD = \begin{array}{l} 0\ , J_t < J_{start} \\ RD_{min} + \left(RD_{max} - RD_{min}\right) \cdot \dfrac{J_t - J_{sow}}{J_{mid} - J_{start}}, J_{sow} \leq J_t < J_{max} \\ D_{root,max}\ , J_t > J_{max} \end{array} \quad (35)$$

where RD_{min} (mm) is the seed depth at sowing time in Julian days J_{sow} (d) and J_{mid} (d) the day at which the plant attains maximum rooting depth, typically at the mid-development stage. Crop development stage duration (L_{stage}) (d) are also provided by Allen et al. (1998) for different crops. The Julian days corresponding to each stage are then given by,

$$J_{stage} = J_{sow} + L_{ini} = J_{dev} \qquad J_{dev} + L_{dev} = J_{mid} \qquad J_{mid} + L_{mid} = J_{late} \qquad J_{late} + L_{end} = J_{end} \quad (36)$$

7 Agronomic model

7.1 Crop cover and height

Crop cover is calculated according to an asymptotic sigmoid function similar to the biomass production function of Hunt (1982), and which uses the degree-day (DD) approach defined as the difference between daily mean temperature and a crop-dependent base temperature for crop development,

$$COV(t) = \frac{COV_{max}}{1 + \frac{COV_{max} - COV_{ini}}{COV_{ini}} \cdot exp(-COV_{max} \cdot f \cdot \frac{\sum DD}{\sum DD_{COV_{max}}})} \quad (37)$$

$$DD_{base} = T - T_{base}, (T \geq T_{base}) \qquad 0, \qquad (T < T_{base}) \quad (38)$$

where,

$COV(t)$: crop cover on day t (%);

COV_{max}: crop dependent maximum crop cover (%);

COV_{ini}: initial crop cover ($0 < COV_{ini} < 1\%$, here 0.5%);

f: shape parameter ($\approx$ 0.07);

DD: degree-day (°C);

$\sum$ DD: sum of DD on day t (since sowing);

$\sum DD_{COV_{max}}$: crop dependent sum of DD since sowing necessary to reach the maximum crop cover (COV_{max});

T: daily mean temperature (°C);

T_{base}: crop dependent minimum daily mean temperature necessary for its development (°C).

We only consider temperature as a limiting factor for crop development; water and nutriments deficits are not accounted for. Crop height, $H_v(t)$, is calculated using the same equation with COV_{max} and C_{ini} replaced by analogous crop height parameters (H_{max} and H_{ini}).

7.2 Topsoil bulk density

Topsoil bulk density has a strong dynamic character on arable land due to tillage, wheel traffic, root development, biological activity, rainfall impacts, shrinking and swelling, freezing and thawing. In this study we address the effects of tillage and rainfall on dry bulk density using methods inspired by those of the WEPP model (Alberts et al., 1995). First, a consolidated soil matrix density (BD_m) is calculated using the pedotransfer functions (PTF) of Saxton and Rawls (2006) as a function of soil texture and soil organic matter content. Then tillage and rainfall effects are taken into account as detailed below.

7.2.1 Bulk density on days with tillage

On days with tillage, the topsoil soil bulk density (BD_t) is calculated as,

$$BD_t = BD_{t-1} - F_d BD_{t-1} + \frac{2}{1+S_{tx}} F_d \frac{3}{4} BD_m \tag{39}$$

where:
BD_m: soil matrix density (g cm^{-3}) obtained from the FTP of Saxton and Rawls (Saxton2006);
BD_{t-1} and BD_t: bulk density at resp. day $t-1$ and day t (g cm^{-3});
F_d: surface fraction disturbed by tillage (-), determined from lookup tables of the WEPP model (Alberts et al., 1995);
S_{tx}: soil texture related parameter accounting for particle cohesion effects (-), with S_{tx} < 1 for sandy soils and > 1 for clayey soils (USDA, 2003). Its value is determined from soil texture classes using lookup tables of the RUSLE model (USDA,2003).

Thus according to equation 39, tillage reduces the bulk density to 75% of the consolidated soil matrix density for silty soils and tillage affecting the entire surface. This factor is based on bulk density measurements directly after tillage compared to values obtained by the end of the growing season before crop harvest.

7.2.2 Bulk density on days without tillage

On rainy days without tillage, rainfall impact on topsoil bulk density is calculated as a function of the bulk density of the day before, the rainfall on day t, a soil stability factor (S_{stab}), wheel track compaction (wt) and soil cover by either vegetation or crop residues according to,

$$BD_{bs,t} = BD_{bs,t-1} + (BD_m - BD_{bs,t-1})(1 - exp(\frac{-R_t}{S_{stab}})) \tag{40}$$

$$BD_{resi,t} = BD_{resi,t-1} + (BD_m - BD_{resi,t-1})(1 - \frac{2 + exp(\frac{R_t}{S_{stab}})}{3}) \quad (41)$$

$$BD_{crop,t} = \frac{BD_{resi,t} + BD_{bs,t}}{2} \quad (42)$$

$$BD_{wt,t} = 1.15 \cdot BD_m \quad (43)$$

where, BD_{bs}, BD_{resi}, BD_{crop}, BD_m (g cm^{-3}) are respectively, topsoil bulk density of bare soil surface parts (bs), parts covered with crop residues (resi), parts covered with living crop (crop), and wheel tracks (wt);

R_t: rainfall on day t (mm);

The soil stability factor S_{stab} (-) is derived from the crusting index of Rémy and Marin-Laflèche (1974) and is defined as:

$$S_{stab} = 1000/I_C \quad (44)$$

$$I_C = 5(I_S - 0.2) \quad (45)$$

$$I_S = \frac{1.5FS + 0.75CS}{Clay + 10SOM} - Y \quad (46)$$

$$Y = 0.2(pH - 7), (pH > 7) \qquad 0, \qquad (pH \leq 7) \quad (47)$$

where:

IS: soil stability index (-);

IC: crusting index (-);

FS: fine silt content (%);

CS: coarse silt content (%);

$Clay$: clay content (%);

SOM: top soil organic matter content (%).

7.3 Characteristic water contents and topsoil saturated hydraulic conductivity

The regression PTFs of Saxton and Rawls (2006) were used to calculate the topsoil water contents at saturation (θ_{sat} at 0 kPa moisture tension), wilting point (θ_{wp} at 1500 kPa) and field capacity (θ_{fc} at 33 kPa) by injecting the above modeled bulk densities per surface type (wheel track, bare soil, residue-covered and crop-covered surfaces). Then for each surface type, the saturated hydraulic conductivity is derived from Saxton and Rawls (2006),

$$K_{sat} = 1930(\theta_{sat} - \theta_{wp})^{3-\lambda} \tag{48}$$

with λ being the slope of the logarithmic tension-moisture curve (-), determined using θ_{fc} and θ_{wp}. The final K_{sat} at the field scale is calculated as the weighted average of K_{sat}, the weight depending on the within-field surface fraction occupied by each of the four surface types.

8 Mass transfer model

8.1 Mass phase distribution

Mass distribution at time t is given by,

$$M_{tot}(t) = V_{gas}c_{gas} + V_{H_2O}(t)c_{aq}(t) + M_{soil}(t)c_{ads}(t) \tag{49}$$

where c_{aq} ($\mu g\ L^{-1}\ H_2O$), c_{ads} (g Kg^{-1} soil), c_{gas} ($\mu g\ L^{-1}$ air) are the dissolved, adsorbed and gaseous S-metolachlor concentrations, respectively and where $c_{ads} = c_{aq}K_d$ and $c_{gas} = c_{aq}/K_H^{cc}$. V_{gas} and V_{H_2O} are the unsaturated and saturated pore space volume (L), respectively and M_{soil} is the soil mass (Kg).

8.2 Volatilisation

Pesticide volatilisation is only considered on the day of application and follows Leistra et al. (2001), where a boundary air layer is conceptualised through which pesticide diffuses before escaping into the atmosphere. The thickness (d_a, m) of this layer, was assumed to be equivalent to the topmost soil layer's thickness (10 mm) and regulates the transport resistance (r_a, d/m) such that:

$$r_a(t) = \frac{d_a}{D_a(t)} \tag{50}$$

where D_a (m^2/d) is the diffusion coefficient in air for Metolachlor at the observed environmental temperature and adjusted relative to the reference diffusion coefficient ($D_{a,r}$, m^2/d) as:

$$D_a(t) = \Big(\frac{T(t)}{T_r}\Big)^{1.75} D_{a,r} \tag{51}$$

where T and T_r are the environmental temperature at time t and at the reference temperature at 293.15°K, respectively.

The total volatilization is given by the flux across the air layer boundary ($J_{v,air}$) and the flux across the topmost soil layer ($J_{v,soil}$) such that:

$$J_{v,air}(t) = -\frac{C_{gas,top}(t) - C_{air}(t)}{r_a} \tag{52}$$

$$J_{v,soil}(t) = -\frac{C_{gas,z_0}(t) - C_{gas,top}(t)}{r_s} \tag{53}$$

where $C_{gas,top}$ (mg/m^3) is the concentration in gas phase at the soil surface, C_{air} (mg/m^3) the concentration in air, C_{gas,z_0} (mg/m^3) the concentration in gas phase at the center of the uppermost soil layer and r_s (d/m) the diffusion resistance across the topmost soil layer and given by:

$$r_s(t) = \frac{0.5 D_z}{D_{rdiff,g}(t)} \tag{54}$$

To calculate the relative diffusion ($D_{rdiff,gas}$, m^2/d) the model provides two options. Under option 1 (Millington and Quirk, 1960),

$$D_{rdiff,gas} = \frac{D_a(t)\Big(\theta_{gas_z}(t)\Big)^a}{\Big(\theta_z(t)\Big)^b} \tag{55}$$

where Jin and Jury (1996) recommend that $a = 2$ and $b = 2/3$. Under option 2 (Currie, 1960),

$$D_{rdiff,gas} = D_a(t)\Big(a\Big)\Big(\theta_{gas_z}(t)\Big)^b \tag{56}$$

where Bakker et al. (1987) recommend $a = 2.5$ and $b = 3$ for moderately aggregated plough layers of loamy soils and humic sandy soils (Leistra et al., 2001).

Finally, it is assumed that flux across both layer boundaries is equivalent ($J_{v,soil} = J_{v,air}$) (Leistra et al., 2001). Considering pesticide concentration in air to be negligble ($C_{air} = 0$), the concentration at the soil surface is:

$$C_{gas,top}(t) = \frac{r_a}{(r_a + r_s)} C_{gas,z_0(t)} \tag{57}$$

The gas concentration in the soil layer is related to the dimensionless Henry constant (K_H), where:

$$C_{gas,z_0}(t) = C_{aq,z_0}(t) K_H \tag{58}$$

Substituting eq. 57 into eq. 52 yields the mass flux lost to the atmosphere ($g/m^2 d$):

$$J_{v,air} = -\frac{C_{gas,z_0}}{(r_a + r_s)} \tag{59}$$

8.3 Runoff mass

The non-uniform mixing-layer model is adapted from Ahuja and Lehman (1983) (see Shi et al., 2011), eq. 1 and p. 1217) and given by:

$$\frac{\partial(EDI \cdot \theta \cdot C_{aq})}{\partial t} = -ROe^{(-\beta_{RO} \cdot D_{z0})} C_{aq} \tag{60}$$

where the Effective Depth of Interaction (EDI) refers to the mixing layer depth (mm), θ is soil moisture $(m^3\ m^{-3})$, RO is run-off (mm) and C_{aq} is concentration in the mixing layer $(g\ L^{-1})$. The parameter β_{RO} is a calibration constant (assuming, $1 \geq \beta > 0$) and where D_{z0} is the depth (mm) of the top-soil layer.

8.4 Leachate mass

Vertical flux can be computed differently across soil layers. Under the first approach, and only for the uppermost layer, the model follows McGrath et al. (2008):

$$C_{z_0,aq}(t+1) = C_{z_0,aq}(t) exp\Big(\frac{-P(t)}{\theta_{z_0}(t) \cdot RET_{z_0}(t) \cdot D_{z_0}}\Big) \tag{61}$$

where the retardation factor, RET_z (-), is given by:

$$RET_z(t) = 1 + \frac{\rho_{b_z}(t) \cdot K_d}{\theta_z(t)} \tag{62}$$

The mass leached (g) is thus given by:

$$M_{z_0,lch}(t) = D_{z_0} \cdot A_i \Big(\theta_{z_0}(t) C_{z_0,aq}(t) - \theta_{z_0}(t+1) C_{z_0,aq}(t+1)\Big) \tag{63}$$

where A is the area (m^2) for each cell i. For subsurface layers (i.e., z > 0), mass leached is proportional to the aqueous concentration in percolated water such that,

$$M_{z,lch}(t) = P_z(t) \cdot C_{z,aq}(t) \cdot A_i \tag{64}$$

8.5 Lateral mass flux

Similarly to vertical mass flux, later mass flux is proportional to lateral water flow and the aqueous concentration at each cell i,

$$M_{z,lf}(t) = LF_{z_i}(t) \cdot C_{z_i,aq}(t) \cdot A_i \tag{65}$$

9 Degradation model

To account for changes in DT50 (days) due to changes in soil moisture, models from Walker (1974) and Schroll et al. (2006) where compared and evaluated against DT50 values derived from microcosm degradation experiments conducted at different temperatures (°C) and moistures ($m^3\ m^{-3}$). Observed DT50 values were: $DT50_{ref} = 30$ at $\theta = 0.2$, $T = 20$ (used as reference for validation); $DT50 = 41$ at $\theta = 0.4$, $T = 20$; $DT50 = 30$ at $\theta = 0.4$, $T = 30$). Although both methods mostly underestimated measured DT50 (Fig. S4), Walker's approach resulted in smaller error differences and was selected for model implementation.

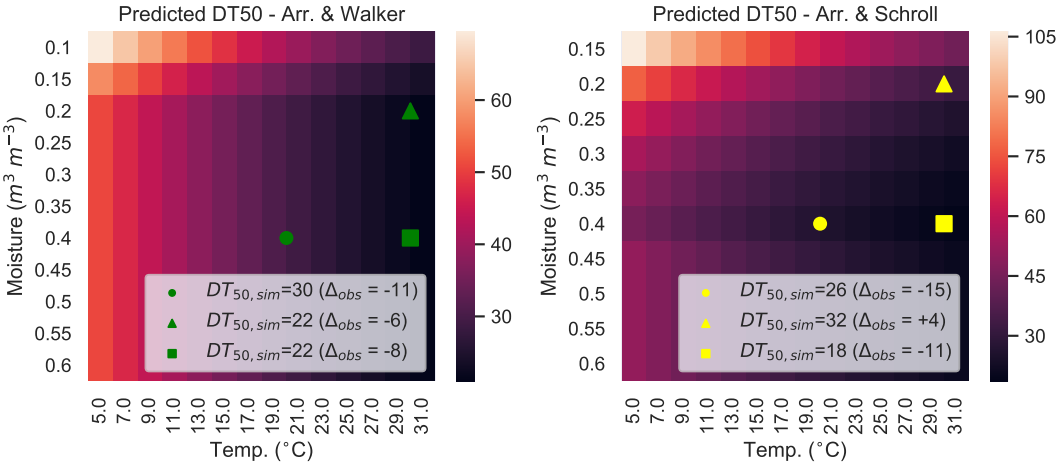

Figure S4. Calculated DT50 from Walker (1974) and Schroll et al. (2006) and differences to observed (Δ_{obs}) DT50 values from S-metolachlor microcosm degradation experiments. Both approaches follow Boesten and van der Linden (1991) for adaptation to the Arrhenius equation.

10 Morris

Morris is a global sensitivity analysis method based on calculation of elementary effects or EEs (see Morris, 1991 and Campolongo et al., 2007). Two sensitivity measures are the mean and SD of the EEs. The mean estimates the overall effect of each parameter on the output and the SD estimates interaction between inputs. Namely, if the mean of a given parameter *i* is different (relatively) from zero, it indicates that parameter *i* has an important "overall" influence on the output. A large SD implies that parameter *i* has a nonlinear effect on the output, or that there are interactions between parameter *i* and other parameters.

Figures S5 and S6 shows sensitivity results for S-metolachlor concentration and isotope signatures (respectively) for outlet and composite transects. Parameters removed from hypercube sampling included water content at -100 cm (W100 all layers); wilting point (all layers: WPz2, WPZ); field capacities and saturation capacities (all layers: SATz2, SATZ).

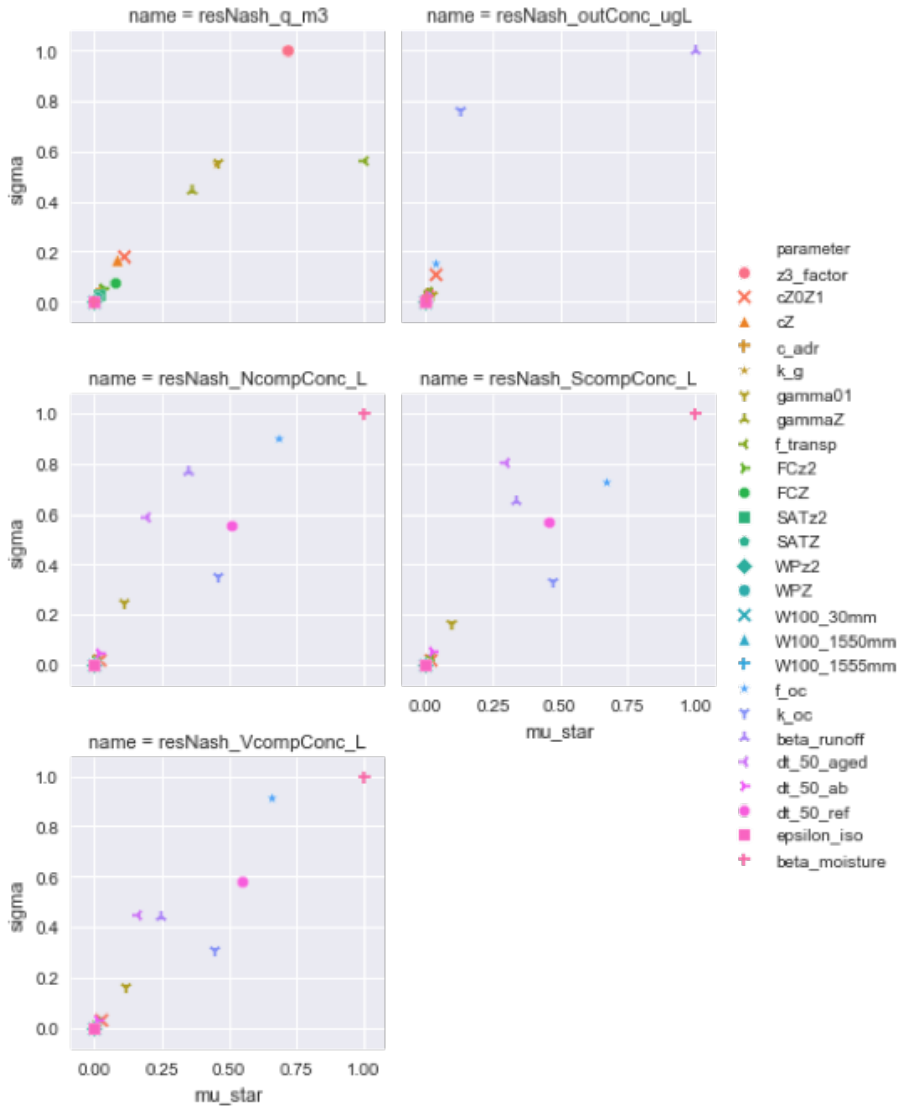

Figure S5. Morris sensitivity results for S-metolachlor concentrations at the outlet (top right) and composite soil transects (North, Valley and South). Discharge sensitivity (m^3) is also shown (top left)

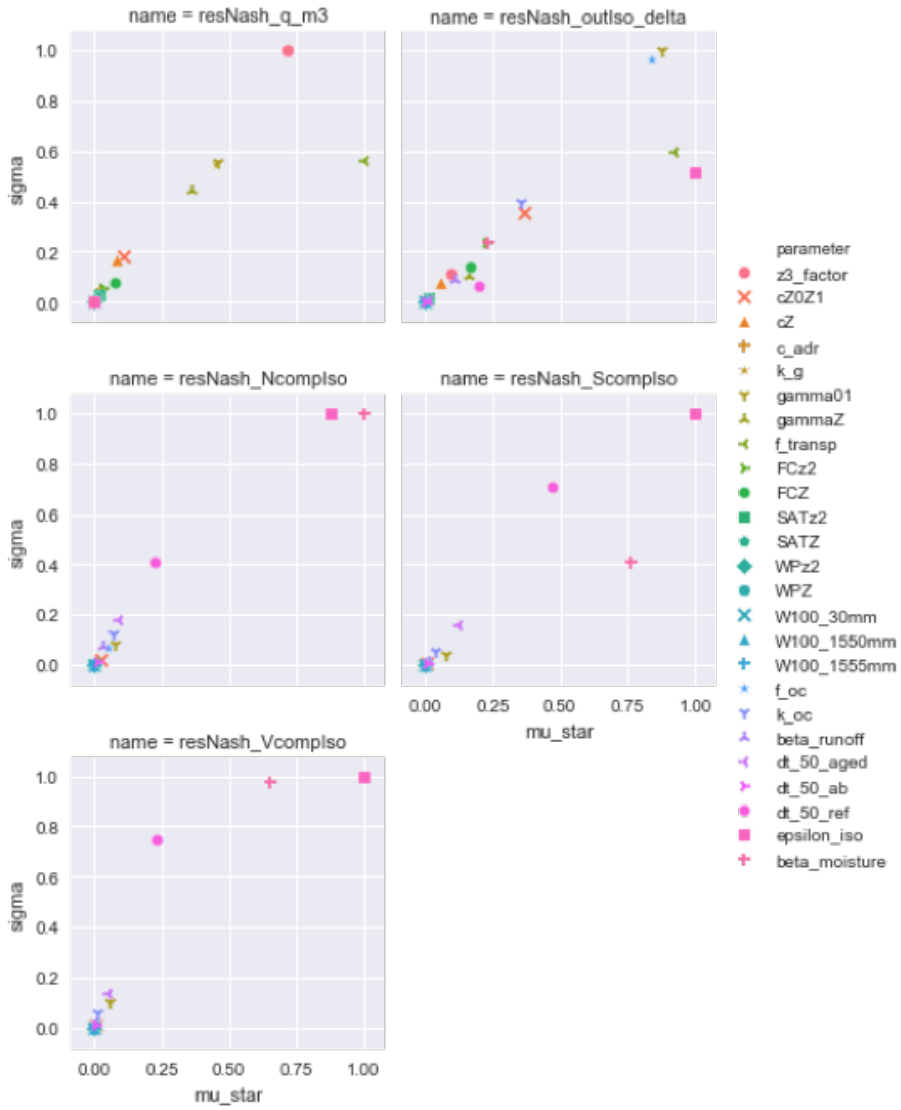

Figure S6. Morris sensitivity results for isotope signatures at the outlet (top right) and composite soil transects (North, Valley and South). Discharge sensitivity (m^3) is also shown (top left)

11 Measured S-metolachlor concentrations and $\delta^{13}C$ for weekly transects

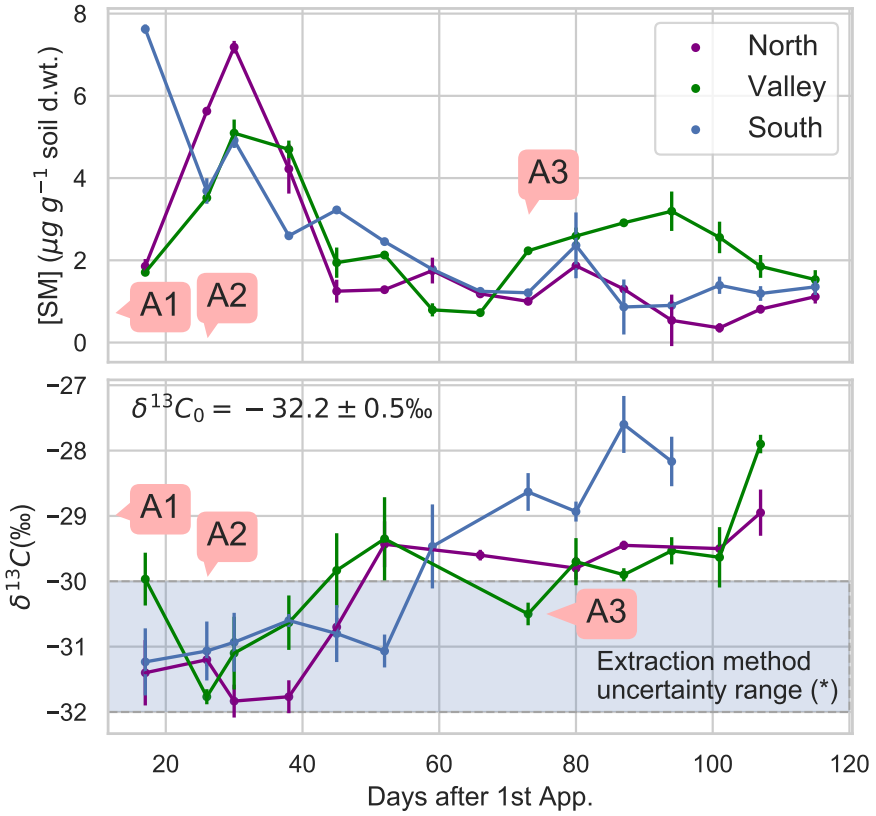

Figure S7. (Top) Measured S-metolachlor concentrations and (Bottom) δ^{13}C for weekly transects. Confirmed applications A1, A2, and A3 (Table S2). (B) Shaded area indicates uncertainty range of the soil extraction method for S-metolachlor δ^{13}C and within which no significant change from the application product's signature ($\delta^{13}C_0$) may be concluded (Alvarez-Zaldivar et al., 2018).

References

Ahuja, L. R. and Lehman, O. R.: The Extent and Nature of Rainfall-soil Interaction in the Release of Soluble Chemicals to Runoff, J. Environ. Qual., 12, 34–40, https://doi.org/10.2134/jeq1983.00472425001200010005x, 1983.

Alberts, E. E., Nearing, M. A., Weltz, M. A., Risse, L. M., Pierson, F. B., Zhang, X. C., Laflen, J. M., and Simanton, J. R.: Chapter 7. The soil component., in: USDA-Water Eros. Predict. Proj. Hillslope Profile Watershed Model Doc. NSERL Rep. 10, July 1995., 1995.

Allen, R. G., Pereira, L. S., Raes, D., and Smith, M.: Crop evapotranspiration: Guidelines for computing crop requirements, Irrig. Drain. Pap. No. 56, FAO, 300, https://doi.org/10.1016/j.eja.2010.12.001, 1998.

Alvarez-Zaldívar, P., Payraudeau, S., Meite, F., Masbou, J., and Imfeld, G.: Pesticide degradation and export losses at the catchment scale: Insights from compound-specific isotope analysis (CSIA), Water Res., 139, 198–207, https://doi.org/10.1016/j.watres.2018.03.061, 2018.

National Center for Biotechnology Information (NCBI). PubChem Compound Database

Bakker, J. W., Boone, F. R., and Boekel, P.: Diffusie van gassen in grond en zuurstofdiffusiecoëfficiënten in Nederlandse akkerbouwgronden (Diffusion of gases in soil and oxygen diffusion coefficients in Dutch arable soils). Rapport 20, ICW, Wageningen, The Netherlands, 1987.

Boesten, J. J. T. I.: Proposal for field-based definition of soil bound pesticide residues, Sci. Total Environ., 544, 114–117, https://doi.org/10.1016/j.scitotenv.2015.11.122, 2016.

Boithias, L., Sauvage, S., Merlina, G., Jean, S., Probst, J. L., and Sánchez Pérez, J. M.: New insight into pesticide partition coefficient Kd for modelling pesticide fluvial transport: Application to an agricultural catchment in south-western France, Chemosphere, 99, 134–142, https://doi.org/10.1016/j.chemosphere.2013.10.050, 2014.

Campolongo, F., Cariboni, J., and Saltelli, A.: An effective screening design for sensitivity analysis of large models, Environ. Model. Softw., 22, 1509–1518, https://doi.org/10.1016/j.envsoft.2006.10.004, 2007. Currie, J. A.: Gaseous diffusion in porous media. 2. Dry granular materials., Br. J. Appl. Phys., 11, 318–324, 1960.

Elsner, M.: Stable isotope fractionation to investigate natural transformation mechanisms of organic contaminants: principles, prospects and limitations., J. Environ. Monit., 12, 2005–31, https://doi.org/10.1039/c0em00277a, 2010.

European Commission: Review report for the active substance S-Metolachlor, EU Commission Health Consumer Protection Directorate General, 2004.

Fenech, C., Rock, L., Nolan, K., Tobin, J., and Morrissey, A.: The potential for a suite of isotope and chemical markers to differentiate sources of nitrate contamination: A review, Water Res., 46, 2023–2041, https://doi.org/10.1016/j.watres.2012.01.044, 2012.

Hunkeler, D., Meckenstock, R. U., Sherwood Lollar, B., Schmidt, T. C., Wilson, J. T., Schmidt, T., and Wilson, J.: A guide for assessing biodegradation and source identification of organic ground water contaminants using compound specific isotope analysis (CSIA), US EPA, Ada, 2008.

Hunt., R.: Plant Growth Curves – The Functional Approach to Plant Growth., edited by: Arnold, E., Cambridge University Press (CUP), London, 248 pp., https://doi.org/10.1017/s0014479700022857, 1982.

Jin, Y. and Jury, W. A.: Characterizing the Dependence of Gas Diffusion Coefficient on Soil Properties, Soil Sci. Soc. Am. J., 60, 66–71, https://doi.org/10.2136/sssaj1996.03615995006000010012x, 1996.

Kollman, W. and Segawa, R.: Interim Report of the Pesticide Chemistry Database, Environmental Protection Agency, US, California, 1995.

Lefrancq, M., Payraudeau, S., Guyot, B., Millet, M., and Imfeld, G.: Correction to Degradation and Transport of the Chiral Herbicide

S-Metolachlor at the Catchment Scale: Combining Observation Scales and Analytical Approaches, Environ. Sci. Technol., 52, 5517–5517, https://doi.org/10.1021/acs.est.8b01118, 2018.

Leistra, M., van der Linden, A. M. A., Boesten, J. J. T. I., Tiktak, A., and van den Berg, F.: PEARL model for pesticide behaviour and emissions in soil-plant systems; Description of the processes in FOCUS PEARL v 1.1.1., Bilthoven, Natl. Inst. Public Heal. Environ. Wageningen, Alterra, Green World Res. RIVM Rep. 711401009/Alterra-rapport 013; 116 blz.; 9 fig.; 1 tab.; 42 ref., 2001.

Lim, K. J., Engel, B. A., Muthukrishnan, S., and Harbor, J.: Effects of initial abstraction and urbanization on estimated runoff using CN technology, J. Am. Water Resour. Assoc., 42, 629–643, https://doi.org/10.1111/j.1752-1688.2006.tb04481.x, 2006.

Manfreda, S., Fiorentino, M., and Iacobellis, V.: DREAM: a distributed model for runoff, evapotranspiration, and antecedent soil moisture simulation, Adv. Geosci., 2, 31–39, https://doi.org/10.5194/adgeo-2-31-2005, 2005.

McGrath, G. S., Hinz, C., and Sivapalan, M.: Modeling the effect of rainfall intermittency on the variability of solute persistence at the soil surface, Water Resour. Res., 44, 1–10, https://doi.org/10.1029/2007WR006652, 2008.

Millington, R. J. and Quirk, J. P.: Transport in porous media, Trans. 7th Int. Congr. Soil Sci., 1, 97–106, 1960.

Morris, M. D.: Factorial sampling plans for preliminary computational experiments, Technometrics, 33, 161–174, https://doi.org/10.2307/1269043, 1991.

Neitsch, S. L., Arnold, J. G., Kiniry, J. R., and Williams, J. R.: Soil and Water Assessment Tool. Theoretical Documentation. Version 2009.Texas Water Resources Institute Technical Report No. 406 Texas A and M University System College Station, Texas, USA. 647 pages, 2011.

Nestler, A., Berglund, M., Accoe, F., Duta, S., Xue, D., Boeckx, P., and Taylor, P.: Isotopes for improved management of nitrate pollution in aqueous resources: Review of surface water field studies, Environ. Sci. Pollut. Res., 18, 519–533, https://doi.org/10.1007/s11356-010-0422-z, 2011.

Prasad, R.: A linear root water uptake model, J. Hydrol., 99, 297–306, https://doi.org/10.1016/0022-1694(88)90055-8, 1988.

Raes, D.: BUDGET: a Soil Water and Salt Balance Model. Reference manual. Version 5.0., Catholic University of Leuven, Leuven, Belgium, 2002.

Rayleigh, L. S.: Theoretical considerations respecting the separation of gases by diffusion and similar processes, Philos. Mag., 42, 493–498, https://doi.org/10.1080/14786449608620944, 1896.

Rémy, J. C. and Marin-Laflèche, A.: L'analyse de terre : réalisation d'un programme d'interprétation automatique., Ann. Agron., 25, 607–632, 1974.

Saxton, K. E. and Rawls, W. J.: Soil Water Characteristic Estimates by Texture and Organic Matter for Hydrologic Solutions, Soil Sci. Soc. Am. J., 70, 1569–1578, https://doi.org/10.2136/sssaj2005.0117, 2006.

Schroll, R., Becher, H. H., Dörfler, U., Gayler, S., Grundmann, S., Hartmann, H. P., and Ruoss, J.: Quantifying the effect of soil moisture on the aerobic microbial mineralization of selected pesticides in different soils, Environ. Sci. Technol., 40, 3305–3312, https://doi.org/10.1021/es052205j, 2006.

Sheikh, V., Visser, S., and Stroosnijder, L.: A simple model to predict soil moisture: Bridging Event and Continuous Hydrological (BEACH) modelling, Environ. Model. Softw., 24, 542–556, https://doi.org/10.1016/j.envsoft.2008.10.005, 2009.

Sherwood Lollar, B., Slater, G. F., Sleep, B., Witt, M., Klecka, G. M., Harkness, M., and Spivack, J.: Stable carbon isotope evidence for intrinsic bioremediation of tetrachloroethene and trichloroethene at Area 6, Dover Air Force Base, Environ. Sci. Technol., 35, 261–269, https://doi.org/10.1021/es001227x, 2001.

Shi, X. N., Wu, L. S., Chen, W. P., and Wang, Q. J.: Solute Transfer from the Soil Surface to Overland Flow: A Review, Soil Sci. Soc.

Am. J., 75, 1214–1225, https://doi.org/DOI 10.2136/sssaj2010.0433, 2011. Soil Conservation Service: Soil Conservation Service. Section
385 4 Hydrology, in: Natl. Eng. Handbook, SCS. Soil, 1972.
USDA: Revised Universal Soil Loss Equation. Version 2. (RUSLE2)., Springer-Verlag, https://doi.org/10.1007/springerreference$_7$7104, 2003.
$Walker, A.: ASimulationModelforPredictionofHerbicidePersistence, J.Environ.Qual., 3, 396˘401, https://doi.org/10.2134/jeq1974.00472425000300040021x, 1974.$